Performance of QS-CDMA over Frequency Selective Time Non-Selective Multipath Generalized Gamma Fading Channels

Ferkan YILMAZ and Oğuz KUCUR
Electronics Engineering Dept., Gebze Institute of Technology, P.K. 141, 41400 Gebze-Kocaeli, Turkey
E-mail: ferkan.yilmaz@gmail.com, okucur@gyte.edu.tr

Abstract-**Direct Sequence (DS) Code Division Multiple Access (CDMA) systems are considered for a variety of wireless applications and services because DS-CDMA enables the transmission of multimedia messages such as voice, data and video. The performance of Quasisynchronous DS-CDMA (QS-CDMA) communication system with a maximal ratio combiner (MRC) over a frequency selective time non-selective multipath Generalized Gamma fading channel is derived for not only any random / deterministic spreading sequences but also any chip-limited chip waveforms. Numerical and simulation results show that the performance of QS-CDMA is as good as or slightly better than synchronous CDMA (S-CDMA) when the maximum quasisynchronous delays do not need to be less than some specific values depending on the path power scattering. With this flexibility of quasisynchronous delays for the better performance, both the transmitter and receiver complexity is reduced as quasisynchronous communication is a challenging task for researchers. Lastly, a measure, Partial Power Ratio (PPR), is defined based on the partial autocorrelation functions, to select or design a chip waveform for quasisynchronous communication. Results show that QS-CDMA using the chip waveform whose PPR is greater, has better performance.**

I. INTRODUCTION

DS-CDMA systems are considered for a variety of wireless applications and services because DS-CDMA enables the transmission of multimedia messages such as voice, data and video over the same channel, and provides high capacity and quality of service. Therefore, it is currently being employed in digital cellular mobile radio communication systems [**1**], [**2**]. However, the system performance is usually limited as a result of multipath environment, fading, the cross-correlation functions of the spreading sequences employed by users, and the maximal allowed delays among the users [**3**], [**4**], [**5**]. Moreover, by increasing number of mobile users, multiple access interference (MAI) considerably degrades the demodulator performance. To alleviate this performance degradation, MAI must be minimized irrespective of channel characteristics [**4**]. Hence, the orthogonal spreading sequences must be employed while the maximal allowed delays among the users are constrained into a small fraction of one chip duration due to the fact that Synchronous CDMA (S-CDMA) has very low MAI over fading channels if orthogonal spreading sequences are employed. In this way, this CDMA system possesses almost all intrinsic advantageous of Synchronous CDMA (S-CDMA). In literature, this type of CDMA is called Quasisynchronous CDMA (QS-CDMA). This problem is first studied in [**4**], [**5**], [**6**]. The exact knowledge of mobile users' delays / amplitudes is very important to improve the performance of QS-CDMA because the elimination of MAI is possible only if the users' delays / amplitudes are estimated correctly [**7**], [**8**]. Application of new signal formats such as using wavelets is also another choice to reduce MAI for quasisynchronous communication [**9**], [**10**].

The bit error rate (BER) of each user in QS-CDMA system is also affected by the channel characteristics. In multipath fading environment, the received signal at the base station is composed of multiple reflections of the transmitted signal which have their own directions of arrivals, amplitudes, phases and delays [**11**], [**12**], [**13**]. The fading can be either flat or frequency selective. In frequency selective fading, Multipath Intensity Profile (MIP) describes the received signal powers of users on all resolvable paths. A series of propagation experiments conducted in typical urban / indoor areas have revealed the multipath nature of the mobile radio channel such that it is common to assume an exponential power delay profile in urban / indoor systems [**11**], [**12**], [**13**], [**14**]. Recently fewer efforts have been made to study the QS-CDMA system performance, based on the more general fading model such as frequency-selective multipath fading channel. BER performance of a QS-CDMA system over a multipath Rayleigh fading channel is evaluated in [**15**]. Quasisynchronous performances of Walsh-Hadamard, QS, Lin-Chang, LCZ-GMW, ZCZ sequences are compared using a conventional receiver (RAKE) and a Parallel Interference Canceller (PIC) receiver over a multipath Rayleigh fading channel [**16**].

However, in this paper, while the symbol error rate (SER) performance of QS-CDMA is derived for M-level Phase Shift Keying (MPSK) signaling over frequency selective time non-selective multipath Generalized Gamma fading channels, a maximal ratio combiner (MRC) is used to recover signals on each resolvable path and combine them in order to increase Signal-to-Noise Ratio (SNR) at the receiver. Firstly, the SER performance is obtained for both any spreading sequences and any chip-limited chip waveforms. Secondly, Numerical and simulation results show that the performance of QS-CDMA will be as good as or slightly better than the performance of S-CDMA when the maximum quasisynchronous delays do not need to be less than such specific values as 0.2 chip period for Rectangular, 0.6 chip period for Half-Sine, and 0.7 chip period for Raised-Cosine chip waveform, depending on the path power scattering function. With this flexibility on the maximum quasisynchronous delay, the receiver synchronization complexity is decreased. Lastly, a measure, which we call Partial Power Ratio (PPR), is defined based on these partial correlation functions to select or design a chip waveform for quasisynchronous communication. Results show that QS-CDMA using the chip waveform whose PPR is greater than that of other chip waveforms, has better performance.

The remainder of this paper is organized as follows. In Section II, we present the transmitter, the multipath fading channel and the receiver models, and maximal ratio combining. In Section III, SER performance is derived. Numerical and simulation results are provided in Section IV, and in the last section, our conclusions are drawn.

II. QS-CDMA SYSTEM MODEL

A. Transmitter Model

We consider an uplink DS-CDMA wireless communication with quasisynchronous channel access model that consists of K users. Users are assigned specific spreading sequences such that they share the same channel resources and transmit with delays smaller than one chip duration. The transmitter schematic of the kth user is shown in Figure 1.

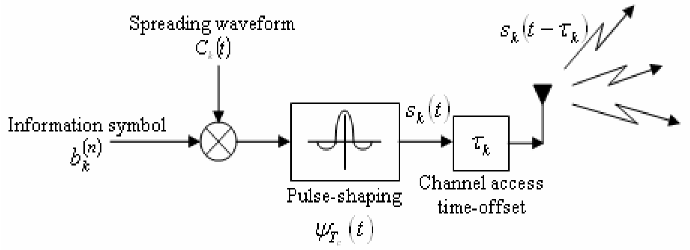

Figure 1. Transmitter structure of user k

The transmitted signal of user k can be represented in terms of time instants nT_b as follows [**4**], [**5**]

$$s_k(t) = \sum_{n=-\infty}^{\infty} \sum_{m=0}^{N-1} \sqrt{P_k}\, b_k^{(n)} C_k^{(m)} \psi_{T_c}\left(t - nT_b - mT_c - \tau_k\right) \qquad (1)$$

where n is the time instant index, T_b is the period of information pulses, and T_c is the chip duration with respect to spreading gain such that $N = T_b / T_c$. P_k and $b_k^{(n)}$ denote the power and information symbols of user k, respectively. $\left\{C_k^{(m)}\right\}_{m=0}^{N-1}$ is the spreading sequence of user k. Spreading waveform of user k is defined as

$$C_k(t) = \sum_{m=0}^{N-1} C_k^{(m)} \psi_{T_c}\left(t - mT_c\right),\ 0 \le t < T_b \qquad (2)$$

where $\psi_{T_c}(t)$ represents arbitrary shape of the chip-limited chip waveform. In this work, the performance expressions are obtained for any chip waveform. However, the following chip waveforms are investigated for simulation and numerical results,

Rectangular $$\psi_{T_c}(t) = \sqrt{\frac{1}{T_c}},\ 0 < t < T_c \qquad (3)$$

Half-Sine $$\psi_{T_c}(t) = \sqrt{\frac{2}{T_c}} \sin\left(\pi \frac{t}{T_c}\right),\ 0 < t < T_c \qquad (4)$$

Raised-Cosine $$\psi_{T_c}(t) = \sqrt{\frac{2}{3T_c}} \left[1 - \cos\left(2\pi \frac{t}{T_c}\right)\right],\ 0 < t < T_c \qquad (5)$$

For quasisynchronous case, the delays among the users are restricted to a small fraction of one chip duration. Hence, channel access time offset of user k can be expressed as $\tau_k = \Delta_k T_c$, where Δ_k is the normalized quasisynchronous delay of user k and is uniformly distributed over $-\Delta_s \le \Delta_k \le \Delta_s$. Δ_s is the maximum allowed quasisynchronous delay between all users such that $0 < \Delta_s < 1$ [**4**], [**5**]. Relative delays between all users influence the system performance. The relative delay of user i with respect to user k is stated as $\hat{\tau}_i = \tau_i - \tau_k$. The relative normalized quasisynchronous delay of user i is expressed as

$$\hat{\Delta}_i = \Delta_i - \Delta_k \qquad (7)$$

which has the triangular probability density function (pdf) as follows [**5**]

$$f_{\hat{\Delta}_i}(\Delta) = \left(1 - \frac{|\Delta|}{\Delta_s}\right)\frac{1}{\Delta_s},\ -\Delta_s \le \Delta \le \Delta_s \qquad (8)$$

B. Multipath Fading Channel Model

In multipath fading environment, the received signal is composed of multiple reflections of the transmitted signal which have their own directions of arrivals, amplitudes, phases and delays [**13**]. A widely accepted model for a frequency-selective time non-selective multipath fading channel is a finite-length tapped delay line with a tap spacing of one chip [**17**], such that its complex low-pass impulse response for user k at time instant nT_b is given by

$$h_k(t) = \sum_{\ell=0}^{L_c-1} h_{k,\ell}^{(n)} \delta\left(t - \ell T_c\right) = \sum_{\ell=0}^{L_c-1} \alpha_{k,\ell}^{(n)} e^{j\phi_{k,\ell}^{(n)}} \delta\left(t - \ell T_c\right) \qquad (8)$$

where L_c (L_c<<N) is the number of paths between user k and receiver base station. The phases $\left\{\phi_{k,\ell}^{(n)}\right\}$ are mutually independent identically distributed random variables and uniformly distributed in the interval [0,2π). L_c multipath attenuations (tap weights) $\left\{\alpha_{k,\ell}^{(n)}\right\}$ are mutually independent Generalized Gamma random variables with pdf given as [**17**]

$$p_k\left(\alpha_{k,\ell}^{(n)}\right) = M\left(\alpha_{k,\ell}^{(n)}, m, \xi, \Omega_{k,\ell}\right),\ m > 1/2,\ \xi \ge 0$$

$$M(R, m, \xi, \Omega) = \frac{2\xi R^{2\xi m-1}}{\Gamma(m)} \left(\frac{m}{\Omega}\right)^m \exp\left(-\frac{mR^{2\xi}}{\Omega}\right) \qquad (9)$$

where $\Gamma(.)$ represents the gamma function, m denotes the fading figure, defined as [**18**]

$$m = E^2\left[\left|\alpha_{k,\ell}^{(n)}\right|^2\right] \Big/ Var\left[\left|\alpha_{k,\ell}^{(n)}\right|^2\right] \tag{10}$$

where $E[.]$ and $Var[.]$ denote expectation and variance operators, respectively. The parameter, ξ in (9) denotes the shape parameter. Such commonly employed fading models as the Rayleigh (m=ξ=1), Nakagami-m (ξ=1), Weibull (m=1), lognormal ($m\rightarrow\infty$, ξ=0), and AWGN ($m\rightarrow\infty$, ξ=1) are special or limiting cases of the generalized gamma distribution. The parameter $\Omega_{k,\ell}$ in (9) is the MIP which describes the received signal powers of user k on the ℓth path. It is common to assume an exponentially decaying MIP in urban and indoor systems [**13**], [**14**]. Exponentially decaying MIP distribution is given by

$$\Omega_{k,\ell} = \Omega_{k,0}\exp(-\rho\ell),\ \rho > 0 \tag{11}$$

where $\Omega_{k,0}$ is the average signal strength of the first resolvable (main) path. The parameter ρ reflects the decaying rate of the average signal path strength.

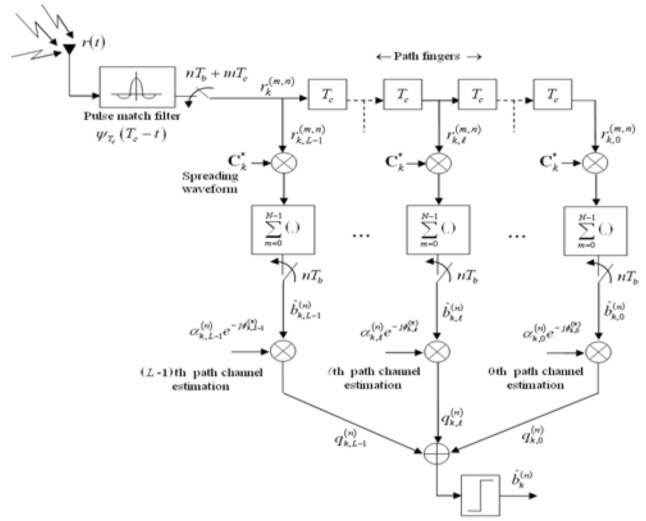

Figure 2. Receiver structure for user k

C. Receiver Model

The total received signal from all users is given as

$$r(t) = \sum_{n=-\infty}^{\infty}\sum_{k=1}^{K}\sum_{m=0}^{N-1}\sum_{\ell=0}^{L-1}\left\{\sqrt{P_k}\,b_k^{(n)}C_k^{(m)}h_{k,\ell}^{(n)} \times \psi_{T_c}\left(t - nT_b - mT_c - \ell T_c - \Delta_k T_c\right)\right\} + n(t) \tag{12}$$

where k, m, ℓ are the indices of users, chips, paths, respectively. The receiver structure for user k at the base station is depicted in Figure 2. $n(t)$ represents the complex AWGN with zero mean and double-sided power spectral density of $N_0/2$. The receiver for user k consists of fingers, each of which is synchronized to different paths. The received signal $r(t)$ is correlated with the chip waveform filter $\psi_{T_c}(T_c - t)$ synchronized to user k, and sampled at time nT_b+mT_c instants, then these samples are delayed by the finite-length tapped delay line (L fingers) with a tap spacing of one chip. The samples at fingers are separately correlated by the spreading sequence of user k, and sampled at time instant nT_b. The recovered samples $\hat{b}_{k,p}^{(n)}$ from the pth finger, $p = 0,\ldots,L-1$, is obtained as

$$\begin{aligned}
\hat{b}_{k,p}^{(n)} = {} & \underbrace{\sqrt{P_k}\,b_k^{(n)}h_{k,p}^{(n)}}_{\text{Desired signal}} + \underbrace{\sum_{\substack{\ell=0\\ \ell\neq p}}^{L_c-1}\sqrt{P_k}\,b_k^{(n)}h_{k,\ell}^{(n)}R_{kk}(p-\ell)}_{\text{ISI resulted from overlapping symbols}} + \\
& \underbrace{\sum_{\substack{\ell=0\\ \ell\neq p}}^{L_c-1}\sqrt{P_k}\,b_k^{(n+[\![p-\ell]\!])}h_{k,\ell}^{(n+[\![p-\ell]\!])}\hat{R}_{kk}(p-\ell)}_{\text{ISI resulted from overlapped adjacent symbols}} + \\
& \underbrace{\sum_{\substack{j=1\\ j\neq k}}^{K}\sum_{\ell=0}^{L_c-1}\sqrt{P_j}\,b_j^{(n)}h_{j,\ell}^{(n)}\left\{R_\psi\left(\hat{\Delta}_jT_c\right)R_{jk}(p-\ell) + \hat{R}_\psi\left(\hat{\Delta}_jT_c\right)R_{jk}\left(p-\ell+[\![\hat{\Delta}_j]\!]\right)\right\}}_{\text{MAI resulted from other mobile users' overlapping symbols}} + \\
& \underbrace{\sum_{\substack{j=1\\ j\neq k}}^{K}\sum_{\ell=0}^{L_c-1}\sqrt{P_j}\,b_j^{(n+[\![p-\ell]\!])}h_{j,\ell}^{(n+[\![p-\ell]\!])} \times \left\{R_\psi\left(\hat{\Delta}_jT_c\right)\hat{R}_{jk}(p-\ell) + \hat{R}_\psi\left(\hat{\Delta}_jT_c\right)\hat{R}_{jk}\left(p-\ell+[\![\hat{\Delta}_j]\!]\right)\right\}}_{\text{MAI resulted from other mobile users' overlapped adjacent symbols}} + \\
& \underbrace{\sqrt{\frac{N_0T_b}{2}}\eta}_{\text{AWGN noise}}
\end{aligned} \tag{13}$$

where $*$ denotes complex conjugation, and $[\![.]\!]$ is sign function. The parameter η is a random variable that reflects the complex AWGN with zero mean and unit variance. $R_{jk}(\ell)$ and $\hat{R}_{jk}(\ell)$ are the partial cross-correlation functions between spreading sequences of users j and k according to overlapping symbols and overlapped adjacent symbols. $R_\psi\left(\hat{\Delta}_jT_c\right)$ and $\hat{R}_\psi\left(\hat{\Delta}_jT_c\right)$ are the partial autocorrelation functions of the chip waveform.

For the L-finger receiver, the decision variable $q_{k,p}^{(n)}$, $p = 1,\ldots,L$, for pth finger at the time instant nT_b is obtained by means of co-phasing and optimally weighting the recovered individual samples $\hat{b}_{k,p}^{(n)}$ with its own fading phase $\phi_{k,\ell}^{(n)}$ and amplitude $\alpha_{k,\ell}^{(n)}$, respectively. The decision random variable for user k, $1 \le k \le K$ is eventually obtained as

$$\hat{b}_k^{(n)} = \sum_{\ell=0}^{L-1} q_{k,\ell}^{(n)}, \tag{14}$$

where $q_{k,\ell}^{(n)}$ is obtained by co-phasing and optimally weighting $\hat{b}_{k,\ell}^{(n)}$ according to the fading of ℓth finger, $q_{k,\ell}^{(n)} = \alpha_{k,\ell}^{(n)}e^{-j\phi_{k,\ell}^{(n)}}\hat{b}_{k,\ell}^{(n)}$.

III. PERFORMANCE ANALYSIS

SER performance of QS-CDMA for MPSK modulation is derived for different chip waveforms and multipath Generalized Gamma fading channels. In the analysis, the statistics of the decision variable, $\hat{b}_k^{(n)}$ seen in Figure 2 is analyzed by using Gaussian approximation such that both MAI and inter symbol interference (ISI) are modeled as an additive Gaussian noise [**20**]. In our approximations, not only spreading gain but also number of users is chosen higher for perfect

Gaussian approximation. Then, SER performance can be obtained by using Gaussian approximation. The decision variable $q_{k,p}^{(n)}$, $p=1,\ldots,L$, of user k, $1\le k\le K$, for pth finger at the receiver at the time instant nT_b can be compactly represented as

$$q_{k,p}^{(n)}=D_{k,p}^{(n)}+ISI_{k,p}^{(n)}+MAI_{k,p}^{(n)}+\eta_{k,p}^{(n)} \tag{15}$$

where the first term, $D_{k,p}^{(n)}$ is the desired signal recovered from the pth finger and expressed as

$$D_{k,p}^{(n)}=\sqrt{P_k}\,b_k^{(n)}\left(\alpha_{k,p}^{(n)}\right)^2 \tag{16}$$

The second term in (15) represents ISI generated from the multipath nature of the channel. It is modeled as Gaussian random variable with zero mean and variance of

$$Var\left[ISI_{k,p}^{(n)}\right]=\left(\alpha_{k,p}^{(n)}\right)^2\sum_{\substack{\ell=0\\ \ell\neq p}}^{L_c-1}P_k\Omega_{k,\ell}Z_{kk}^{I}\left(p-\ell\right) \tag{17}$$

The third term in (15) represents MAI generated from other users' signals, and is also modeled as Gaussian random variable with zero mean and variance of

$$\begin{aligned}Var\left[MAI_{k,p}^{(n)}\right]=\left(\alpha_{k,p}^{(n)}\right)^2\Bigg\{&E\left[R_\psi^2\left(\hat{\Delta}_jT_c\right)\right]\sum_{\substack{j=1\\ j\neq k}}^{K}\sum_{\ell=0}^{L_c-1}P_j\Omega_{j,\ell}Z_{jk}^{I}\left(p-\ell\right)+\\ &2E\left[R_\psi\left(\hat{\Delta}_jT_c\right)\hat{R}_\psi\left(\hat{\Delta}_jT_c\right)\right]\sum_{\substack{j=1\\ j\neq k}}^{K}\sum_{\ell=0}^{L_c-1}P_j\Omega_{j,\ell}Z_{jk}^{II}\left(p-\ell\right)+\\ &E\left[\hat{R}_\psi^2\left(\hat{\Delta}_jT_c\right)\right]\sum_{\substack{j=1\\ j\neq k}}^{K}\sum_{\ell=0}^{L_c-1}P_j\Omega_{j,\ell}Z_{jk}^{III}\left(p-\ell\right)\Bigg\}\end{aligned} \tag{18}$$

where $E\left[R_\psi^2\left(\hat{\Delta}T_c\right)\right]$, $E\left[\hat{R}_\psi^2\left(\hat{\Delta}T_c\right)\right]$ and $E\left[R_\psi\left(\hat{\Delta}T_c\right)\hat{R}_\psi\left(\hat{\Delta}T_c\right)\right]$ are the expected partial powers of chip waveform and correlation between partial autocorrelation functions, respectively. The fourth term in (15) represents the AWGN noise with zero mean and variance of

$$Var\left[\eta_{k,p}^{(n)}\right]=\left(\alpha_{k,p}^{(n)}\right)^2\frac{N_0T_b}{2} \tag{19}$$

In (17) and (18), $Z_{jk}^{I}(\ell)$, $Z_{jk}^{II}(\ell)$ and $Z_{jk}^{III}(\ell)$ are the auxiliary squared correlation functions between any two mobile users (user j and user k), based on the partial cross-correlation functions of spreading sequences, and expressed as

$$Z_{jk}^{I}\left(\ell\right)=R_{jk}^2\left(\ell\right)+\hat{R}_{jk}^2\left(\ell\right) \tag{20}$$

$$\begin{aligned}Z_{jk}^{II}\left(\ell\right)=\frac{1}{2}\Re\Big\{&R_{jk}\left(\ell-1\right)R_{jk}^*\left(\ell\right)+\hat{R}_{jk}\left(\ell-1\right)\hat{R}_{jk}^*\left(\ell\right)+\\ &R_{jk}\left(\ell+1\right)R_{jk}^*\left(\ell\right)+\hat{R}_{jk}\left(\ell+1\right)\hat{R}_{jk}^*\left(\ell\right)\Big\}\end{aligned} \tag{21}$$

$$Z_{jk}^{III}\left(\ell\right)=\frac{1}{4}\Re\left\{R_{jk}^2\left(\ell-1\right)+\hat{R}_{jk}^2\left(\ell-1\right)+R_{jk}^2\left(\ell+1\right)+\hat{R}_{jk}^2\left(\ell+1\right)\right\} \tag{22}$$

where $\Re\{\cdot\}$ denotes the real part. Consequently, upon utilizing the central limit theorem, we obtain the SNR for the decision variable $q_{k,p}^{(n)}$ of pth finger at the receiver as follows

$$\gamma_{k,p}^{(n)}=\frac{E\left[q_{k,p}^{(n)}\right]^2}{Var\left[q_{k,p}^{(n)}\right]}=\frac{\left(D_{k,p}^{(n)}\right)^2}{Var\left[q_{k,p}^{(n)}\right]}=\gamma_{k,p}\left(\alpha_{k,p}^{(n)}\right)^2 \tag{23}$$

where $\gamma_{k,p}$ is the normalized SNR with respect to the squares of the fading amplitudes on the pth resolvable path, and obtained for *any random / deterministic spreading sequences* and *any chip-limited chip waveforms* as follows

$$\begin{aligned}\gamma_{k,p}=P_k\Bigg\{&\sum_{\substack{\ell=0\\ \ell\neq p}}^{L_c-1}P_k\Omega_{k,\ell}Z_{kk}^{I}\left(p-\ell\right)+\\ &E\left[R_\psi^2\left(\hat{\Delta}_jT_c\right)\right]\sum_{\substack{j=1\\ j\neq k}}^{K}\sum_{\ell=0}^{L_c-1}P_j\Omega_{j,\ell}Z_{jk}^{I}\left(p-\ell\right)+\\ &2E\left[R_\psi\left(\hat{\Delta}_jT_c\right)\hat{R}_\psi\left(\hat{\Delta}_jT_c\right)\right]\sum_{\substack{j=1\\ j\neq k}}^{K}\sum_{\ell=0}^{L_c-1}P_j\Omega_{j,\ell}Z_{jk}^{II}\left(p-\ell\right)+\\ &E\left[\hat{R}_\psi^2\left(\hat{\Delta}_jT_c\right)\right]\sum_{\substack{j=1\\ j\neq k}}^{K}\sum_{\ell=0}^{L_c-1}P_j\Omega_{j,\ell}Z_{jk}^{III}\left(p-\ell\right)+\frac{N_0T_b}{2}\Bigg\}^{-1}\end{aligned} \tag{24}$$

In (23), since $\alpha_{k,p}^{(n)}$ is Generalized Gamma random variable mutually independent from the fading amplitudes of other resolvable paths, the *pdf* of $\gamma_{k,p}^{(n)}$ is expressed as [**17**]

$$\begin{aligned}&p_\gamma\left(\gamma_{k,p}^{(n)}\right)=G\left(\gamma_{k,p}^{(n)},m,\xi,\bar{\gamma}_{k,p}\right),\\ &G\left(R,m,\xi,\bar{R}\right)=\xi\left(\frac{\beta}{\bar{R}}\right)^{m\xi}\frac{R^{\xi m-1}}{\Gamma(m)}\exp\left(-\left(\frac{\beta R}{\bar{R}}\right)^{\xi}\right),\ R,\bar{R}>0\end{aligned} \tag{25}$$

where $\beta=\Gamma(m+1/\xi)/\Gamma(m)$ and $\bar{\gamma}_{k,p}$ is the average SNR for the pth resolvable path which is given as

$$\bar{\gamma}_{k,p}=E\left[\gamma_{k,p}\left(\alpha_{k,p}^{(n)}\right)^2\right]=\gamma_{k,p}\Omega_{k,p} \tag{26}$$

The number of fingers at the MRC receiver is formerly chosen as L according to the desired channel resolution, the receiver complexity and multipath delay spread. Finally, the SNR of the decision random variable $\hat{b}_k^{(n)}$ at the time instant nT_b for user k, $1\le k\le K$, can be reduced to the sum of SNRs of the finger decision variables $q_{k,p}^{(n)}$, $p=0,1,\ldots,L-1$ [**21**], given by

$$\gamma_k^{(n)}=\sum_{p=0}^{L-1}\gamma_{k,p}^{(n)}=\sum_{p=0}^{L-1}\gamma_{k,p}\left(\alpha_{k,p}^{(n)}\right)^2 \tag{27}$$

Having obtained the statistics of the finger decision variables, we can derive SER for QS-CDMA over frequency selective time non-selective multipath Generalized Gamma fading channels. For MPSK signaling, the SER conditioned on a set of SNRs of the resolvable paths is then expressed as [**21**]

$$P_{k,SER}^{(n)}\left(\gamma_{k,0}^{(n)},\ldots,\gamma_{k,L-1}^{(n)}\right)=\frac{1}{\pi}\int_0^{(M-1)\pi/M}\exp\left(-\frac{\sin^2\left(\pi/M\right)}{2\sin^2\theta}\sum_{p=0}^{L-1}\gamma_{k,p}^{(n)}\right)d\theta \tag{28}$$

Since the power strengths $\gamma_{k,p}^{(n)}$, p=1,..,L-1 of resolvable paths are mutually independent but not identically distributed, the conditioned SER can be averaged over the pdf of each $\gamma_{k,p}^{(n)}$. Then, SER performance is obtained as

$$P_{k,SER}=\int_0^\infty\cdots\int_0^\infty P_{k,SER}^{(n)}\left(\gamma_{k,0}^{(n)},\ldots,\gamma_{k,L-1}^{(n)}\right)\prod_{p=0}^{L-1}p_{\gamma_\ell}\left(\gamma_{k,p}^{(n)}\right)d_{\gamma_{k,0}^{(n)}}\ldots d_{\gamma_{k,L-1}^{(n)}} \tag{29}$$

Consequently, in terms of Fox's H functions [**22**], SER performance is derived as follows

$$P_{k,SER} = \frac{1}{\pi} \int_{0}^{\frac{\pi(M-1)}{M}} \prod_{p=0}^{L-1} \frac{1}{\Gamma(m)} \mathrm{H}_{1,1}^{1,1}\left[\frac{\bar{\gamma}_{k,p} \sin^2(\pi/M)}{2\beta \sin^2(\theta)} \middle| \begin{matrix} (1-m, 1/\xi) \\ (0,1) \end{matrix} \right] d\theta \tag{30}$$

where $\bar{\gamma}_{k,p}$, given in (26) and (24), will change for different users using deterministic spreading sequences. Therefore, the overall performance of the system is obtained as

$$P_{SER} = \frac{1}{K} \sum_{k=1}^{K} P_{k,SER} \tag{31}$$

IV. NUMERICAL RESULTS

In this section, we evaluate (31) and do computer simulations for the SER performance of QS-CDMA with MRC combiner and MPSK signaling over frequency selective time non-selective Generalized Gamma fading multipath channels and investigate the effects of chip waveform shaping and maximum normalized quasisynchronous delay (Δ_s) on the system performance. The parameters common in all figures are summarized as follows. The type of spreading sequence, and the spreading gain are chosen Hadamard (Walsh) and $N = 32$ for all users, respectively. And also, the number of resolvable paths of the multipath channel is chosen as L_c=10. The power decaying rate changes from 1 to 4 for almost indoor communication. The systems are fully loaded such that the number of users in the system is K=N, and the powers of users are equal, P_k=P, k=1,..,K.

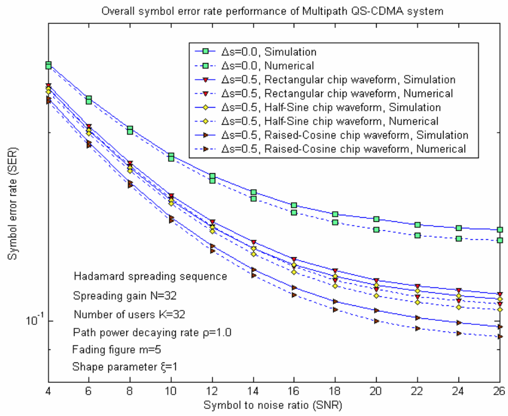

Figure 3. The overall QPSK SER performance of multipath QS-CDMA with five-finger MRC receiver for maximum quasisynchronous delay Δ_s=0.5 chip.

The overall SER performances of QS-CDMA for Rectangular, Half-sine and Raised-Cosine chip waveforms are depicted in Figure 3. The quasisynchronous performance is interestingly better than the synchronous performance for multipath channels. Moreover, Raised-Cosine chip waveform has the best performance, which can also be, as an innovation, verified *without doing any SER computations / simulations* by the fact that the PPR of Raised-Cosine is higher than those of other chip waveforms. We define PPR as follows

$$PPR = \frac{E\left[R_{\psi}^{2}\left(\hat{\Delta} T_c\right) \right]}{E\left[\hat{R}_{\psi}^{2}\left(\hat{\Delta} T_c\right) \right]} \tag{31}$$

As seen in Figure 4, the PPR value of the Raised-Cosine chip waveform is the largest among the chip waveforms, which means that the performance of Raised-Cosine chip waveform is better. This result is also seen from Figure 3 and known in literature, however, we provide a measure, PPR to determine that.

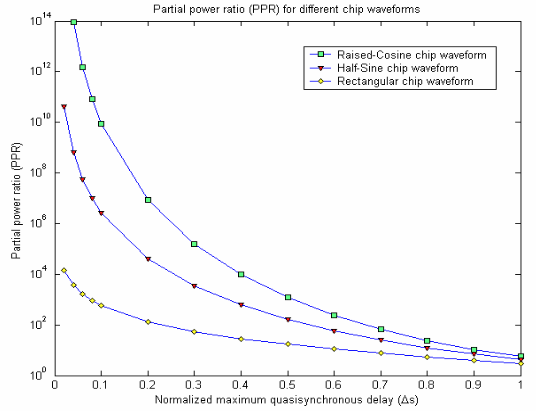

Figure 4. Partial power ratio (PPR) with respect to normalized maximum quasisynchronous delay (Δ_s).

Consequently, PPR can be employed to search suitable chip waveforms for better performance. For instance, one chip waveform can be dependent on some parameters as follows

$$\psi_{T_c}(t) \equiv \psi_{T_c}(\mathbf{x}, t) \tag{32}$$

where $\mathbf{x} = [x_1, x_2, \ldots x_P]$ is the chip waveform shaping parameter vector and P is the length of this parameter vector. The chip waveform for the best performance can be designed / selected by minimizing PPR as follows

$$\hat{\psi}_{T_c}(t) \triangleq \left\{ \psi_{T_c}(\mathbf{x}, t) \middle| \max_{x_1, x_1, \ldots x_P} \frac{E\left[R_{\psi}^{2}\left(\mathbf{x}, \hat{\Delta} T_c\right) \right]}{E\left[\hat{R}_{\psi}^{2}\left(\mathbf{x}, \hat{\Delta} T_c\right) \right]} \right\} \tag{33}$$

Moreover, the power spectral density of chip waveform can also be considered as a constraint for this optimization problem. For asynchronous case, all chip waveforms have similar performance since the PPR values of all chip waveforms are very close for Δ_s=1.0 chip (almost asynchronous case) as seen in Figure 4. However, the performance difference can be better observed when quasisynchronous delays are lower than one chip. Therefore, it is shown by means of PPR that chip waveform design is more suitable for quasisynchronous delays lower than one chip.

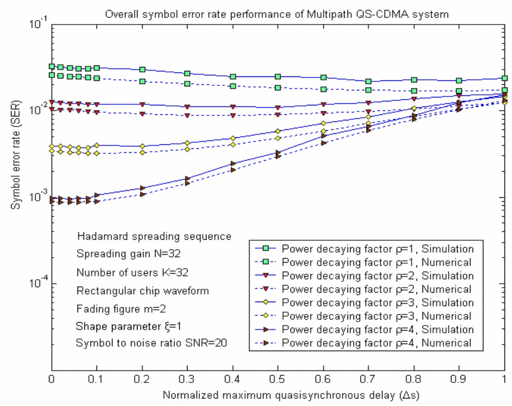

Figure 5. The overall BPSK SER performance of multipath QS-CDMA with Rectangular chip waveform and five-finger MRC receiver.

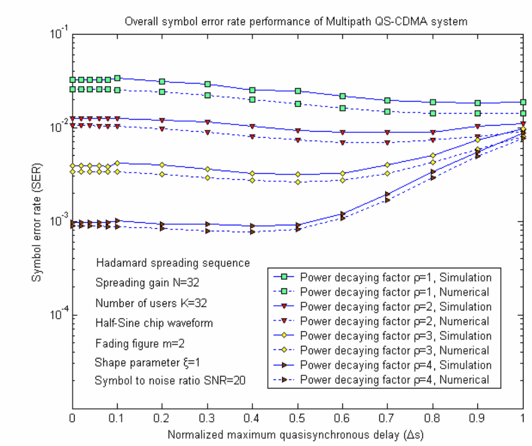

Figure 6. The overall BPSK SER performance of multipath QS-CDMA with Half-Sine chip waveform and five-finger MRC receiver.

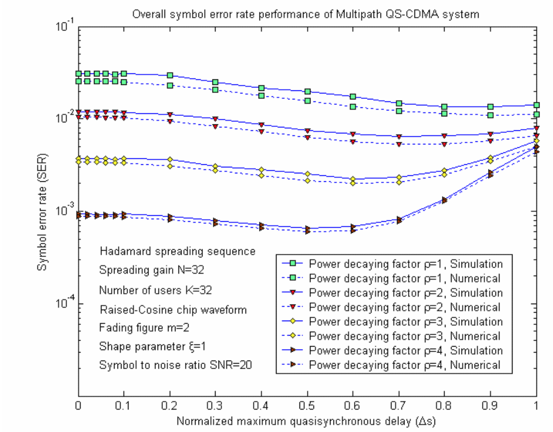

Figure 7. The overall BPSK SER performance of multipath QS-CDMA with Raised-Cosine chip waveform and five-finger MRC receiver.

As seen in Figures 5-7, the performance of the system is still very good, furthermore, better than that of the synchronous communication as long as maximum quasisynchronous delay is lower than the specific values such as 0.2, 0.6, and 0.7 chip period for Rectangular, Half-Sine and Raised-Cosine chip waveforms, respectively, for the power decaying rate ρ=3.0. *Therefore, for better performance, the quasisynchronous delays do not need to be less than these specific values.* More complicated timing algorithms, which complicate the transmitter and receiver structures, to minimize maximum quasisynchronous delays are not needed. Thus, the complexity of quasisynchronous synchronization circuits at both transmitter and receiver are reduced as quasisynchronous communication is a challenging task for researchers.

V. CONCLUSIONS

In this paper, the performance of QS-CDMA in the frequency selective time non-selective multipath Generalized Gamma fading channels has been investigated and the effect of maximum quasisynchronous delays on the performance is addressed. Numerical and simulation results have revealed that the performance of QS-CDMA will be approximately the same as the synchronous performance of QS-CDMA if the maximum quasisynchronous delays are less than specific values which enable wireless network designers some flexibility. In addition, PPR is defined based on the partial correlation functions in order to select or design a chip waveform for quasisynchronous communication. Results show that QS-CDMA using the chip waveform with greater PPR has better performance.

REFERENCES

[1] P. Chaudhury, W. Mohr, and S. Onoe, “The 3GPP Proposal for IMT-2000”, IEEE Communication Magazine, pp. 72-81, Dec.1999.

[2] K.S. Gilhousen, I. M. Jacobs, R. Padovani and L. A. Weaver, “Increased capacity using CDMA for mobile satellite communication”, IEEE Journal on Selected Areas in Communication, vol. 8 pp. 503-514, 1990.

[3] R. Price and P. E. Green, “A Communication Technique for Multipath Channels,” *Proc. IRE*, vol. 46, pp. 555-570, Mar. 1958.

[4] R. De Gaudenzi, C. Ellia and R. Viola, “Bandlimited quasi-synchronous CDMA: A novel satellite access technique for mobile and personal communication systems,” IEEE Journal on Selected Areas in Communications, vol 10, pp. 328-343, Feb. 1992.

[5] V. M. DaSilva and E. S. Sousa, “Multicarrier orthogonal CDMA signals for quasi-synchronous communication systems,” IEEE J. on Selected Areas in Com., vol. 12, pp.842-852, Jun. 1994.

[6] S. Kuno, T. Yamazato, M. Katayama, and A. Ogawa, “A study on quasi-synchronous CDMA based on selected PN signature sequences,” Spread Spectrum Techniques and Applications, vol.2 pp.479-483, July 1994.

[7] R. Iltis, “Exact and approximate maximum-likelihood parameter estimation for quasi-synchronous CDMA signals,” IEEE Transactions on Communications, vol. 48, no. 7, pp. 1208-1216, July 2000.

[8] L. Mailaender, and R. Iltis, “Multiuser detectors with single-user parameter estimation on quasi-synchronous CDMA channels”, IEEE Transactions on Communications, vol. 48, no. 2, Feb. 2000.

[9] E. Öztürk, O. Kucur, G.E. Atkin, Performance of optimum wavelet waveform for DS-CDMA chip waveform over QS-AWGN channel, International Journal of Comm. Systems, vol. 19, pp. 1-16, Feb. 2006.

[10] F. Yılmaz, O. Kucur, “Performance of Quasisynchronous Scale-Time Code Division Multiple Access over AWGN channel,” Accepted to Journal of Computers and Electrical Engineering (CEE). To be published.

[11] G. Turin, F. Clapp, T. Johnston, S. Fine, and D. Lavry, “A statistical model of urban multipath propagation,” IEEE Trans. Veh. Technol., vol. VT-21, no. 1, pp.1–9, 1972.

[12] H. Suzuki, “A statistical model for urban radio propagation,” IEEE Trans. Commun., vol. COMM-25, pp. 673–679, July 1977.

[13] J. K. Carves, “Mobile channel characteristics,” Hingham, MA: Kluwer Academic Publishers, 2000.

[14] A.A.M. Saleh, R.A. Valenzuela, “A statistical model for indoor multipath propagation,” IEEE Journal on Selected Areas in Communications, vol. SAC-5, no. 2, pp. 128-137, Feb. 1987.

[15] B.Q. Long, P. Zhang, “The analysis of a generalized QS-CDMA system over a multipath Rayleigh fading channel,” IEEE Wireless Communication System Symposium, pp. 137 – 141, Nov. 1995.

[16] A. Kuramoto, T. Abrao, P.J. Jeszensky, “Sets of sequences for QS-CDMA systems with interference cancellation over multipath Rayleigh fading channels,” Spread Spectrum Techniques and Applications, pp. 694- 698, Aug. 2004.

[17] A. J. Coulson, A. G. Williamson, and R. G. Vaughan,“Improved fading distribution for mobile radio”, IEE Proc. Part F – Comm., vol. 145, no.13, pp. 197-202, June 1998.

[18] M.S. Alouini, A.J. Goldsmith , “A unified approach for calculating error rates of linearly modulated signals over generalized fading channels,” IEEE Transac. on Com. Vol. 47, pp:1324-1334, Sept. 1999.

[19] L. S. Gordon, Principles of Mobile Communication, 2nd Ed. Norwell, MA: Kluwer Academic Publishers, 2001

[20] M.B. Pursley, “Performance evaluation for phase coded spread-spectrum multiple-access communications – Part I: System analysis,” IEEE Trans. on Com., vol. 25, pp. 795-799, Aug. 1977.

[21] M.K. Simon, M.S. Alouine, Digital Communication over Fading Channels, 1st Ed. John Wiley & Sons, Inc.

[22] A.M. Mathai and R.K. Saxena, The H-function with Applications in Statistics and Other Disciplines, John Wiley and Sons, New York, 1978.